Nigerian Journal of Engineering Science Research (NIJESR).
Vol. 6, Issue 4, pp.33-47, December, 2023

ISSN: 2636-7114
Journal Homepage: https://www.iuokada.edu.ng/journals/nijesr/

Investigation of the Effects of Flow Rate on Velocity and Pressure Head using Venturi Flow Meter

[1a]*Olodu D. D. and [1b]Ojarigho E.V.

[1]Department of Mechanical Engineering, Benson Idahosa University, Benin City, Edo State, Nigeria

[a] dolodu@biu.edu.ng; [b]eojarigho@biu.edu.ng

**Corresponding Author: Olodu Dickson David; dolodu@biu.edy.ng* (+2348065325363)

Manuscript History
Received: 26/11/2023
Revised: 27/12/2023
Accepted: 29/12/2023
Published: 30/12/2023

Abstract: *This study focused on investigation of the effects of flow rate on velocity and pressure head using venturi flow meter. The H5 bench venturi flow meter was used in the experimental investigation to characterize the measurement of flow rate in a pipe and improve the computation of the flow rate, velocity head and pressure head. Obtained results show that the mean flow rate, velocity, velocity head, pressure head and time of fluid flow were 0.0002982m³/s, 2.3350m/s, 45.383mm, 28.0417mm and 33.083seconds respectively, while their Standard Error Mean were 0.00002516 m³/s, 0.71741m/s, 17.6885mm, 4.56812mm and 3.0128seconds respectively. The interaction between time and pressure head, time and velocity head, time & flow rate shows a strong negative correlation of -0.696, -0.790 and -0.980 respectively at significance values of 0.124, 0.061 and 0.001. While the interaction between flow rate & velocity head, flow rate & pressure head, velocity & velocity head, velocity & pressure head, velocity head & pressure head, time & flow rate, and flow rate & velocity shows a strong positive correlation of 0.885, 0.725, 0.936, 0.966, 0.845 and 0.819 respectively at significance values of 0.019, 0.103, 0.006, 0.002, 0.034 and 0.046. These results showed that the flow rate of fluid contributes significantly to both the pressure and velocity head of flow. The venturi meter analyses show the relationship between pressure losses and variation of pressure and velocity at different cross-sectional area of the piping system used in transportation of fluid especially in the oil and gas industry.*

Keywords: *Piping System, Pressure Head, Velocity Head, Venturi Flow Meter, Flow Rate*

INTRODUCTION

In fluids with no energy exchange, energy manifests as pressure, velocity, and elevation because of heat transfer, viscous dissipation, or shaft work (pump or other device). Daniel Bernoulli (1700–1782) first proposed the connection between these three types of energy on the basis of the conservation of energy principle.

Three presumptions underpin Bernoulli's theorem regarding flow streamlines: steady flow, incompressible fluid, and absence of fluid friction losses. In this experiment, the validity of Bernoulli's equation was investigated. Clemens Herschell initiated and created the venturi meter in 1887 (Demirkesen *et al.,* 2020). Since then, venturi meter has proven to be widely applicable in the oil and gas sector for large pump flows and energy conservation (Elperin *et al.,* 2012). Venturi stands out from other flow meters due to its low head loss, which makes it easy to distinguish from orifice flow meters. It is also used in two-phase and slurry flows. Additionally, according to Aichouni *et al.* (2016), a venturi meter is thought to have a high coefficient of discharge, or performance that approaches the theoretical value. As a result, the sensitivity of flow meters to their operating conditions is a major concern for both end users and flow meter manufacturers. Analysis of their data showed that there are large financial losses, and the error brought on by the distorted-abnormal flow meter internal conditions can be very significant (Aichouni *et al.,* 2016). Various studies have been conducted in the public domain to enhance flowmeter performance. It is crucial to have a fundamental understanding of how low-meter operating conditions affect the coefficient of discharge in order to minimize or completely eradicate installation effects that could otherwise lower flow meter accuracy. An experimental investigation on the impact of severely distorted flow conditions on a venturi flow meter's accuracy was carried out by Archouni *et al.* (2020). The findings demonstrate that severely distorted flow conditions may be the source of the required error in the meter reading. Joseph (2018) provided an experimental demonstration of the possible influence of these effects on the venturi meter reading. Analogously, Aichouni *et al.* (2016) carried out an experimental study to examine the impact of installation on the performance of venturi flow meters. The findings show that errors brought on by unusual operating circumstances can result in sizable financial losses. Using steady-state flow benches, Deo and Tiwari (2008) presented their experimental work on the in-cylinder flow of an internal combustion engine (ICE). The obtained results demonstrate that the impulse torque meter method and paddle wheel technique were able to achieve a reasonable level of agreement. Demirkesen *et al.* (2020) presented the results of an experimental and numerical investigation into the air flow motion in the cylinders of heavy-duty diesel engines. Their research shows that the compressive ratio in cylinders is significantly impacted by surface quality and possibly production issues. According to Shinde *et al.* (2020), they developed a model for gas which dissolved in the liquid phase involved in a two-phase flow through a venture tube. The model developed was used to predict pressure drop. Their results show that the analytical solution can be used to estimate the flow conditions. According to Shinde *et al.* (2020), a model was also created using simulation and computational fluid dynamics (CFD) to investigate venturi parameters and calculate the coefficient of discharge. Using computational fluid dynamics, Sanghani *et al.* (2016) investigated the impact of various geometrical parameters on pressure drop in venturi meters, including throat length, diameter ratio, divergent cone angle, and convergent cone angle (Gupta *et al.,* 2018). Their research's primary goal is to determine the critical factors that influence the venturi flow meter's economic losses and to suggest ways to lower those losses for the oil and gas sectors (Muhammad *et al.,* 2021). Thus, the purpose of this study is to ascertain how the internal conditions of a distorted and abnormal flow meter affect the venture meter's reading dynamically. The differential pressure obtained through the venturi meter will be used to calculate the error flow rate with the discharge coefficient shift (Guria *et al.,* 2016).

MATERIALS AND METHOD

2.1. Materials

The following equipment was used in this study.

A. Equipment

To finish the demonstration of the Bernoulli equation experiment, the following tools were used in this research work: i. a stopwatch for timing the flow measurement; ii. test equipment for the Bernoulli apparatus (F1-15); and iii. an F1-10 hydraulic bench.

B. Equipment Description

A tapered duct (venturi meter), a number of manometers tapped into the venturi to measure the pressure head, and a hypodermic probe that can be moved along the test section's center to measure the total head make up the Bernoulli test apparatus (Hall *et al.,* 2017). The test section consists of a circular duct with variable diameter that is inclined at one side to a 14° angle and at another to a 21° angle. Manometers can be connected to the test section using a series of side-hole pressure tappings that are offered (Fig. 1).

2.2. Method

Using a tapered duct (venturi system) coupled with the manometers to measure the velocity head, pressure head, and total head at known points along the flow. This experiment tested the validity of Bernoulli's equation (Sanghani *et al.,* 2016).

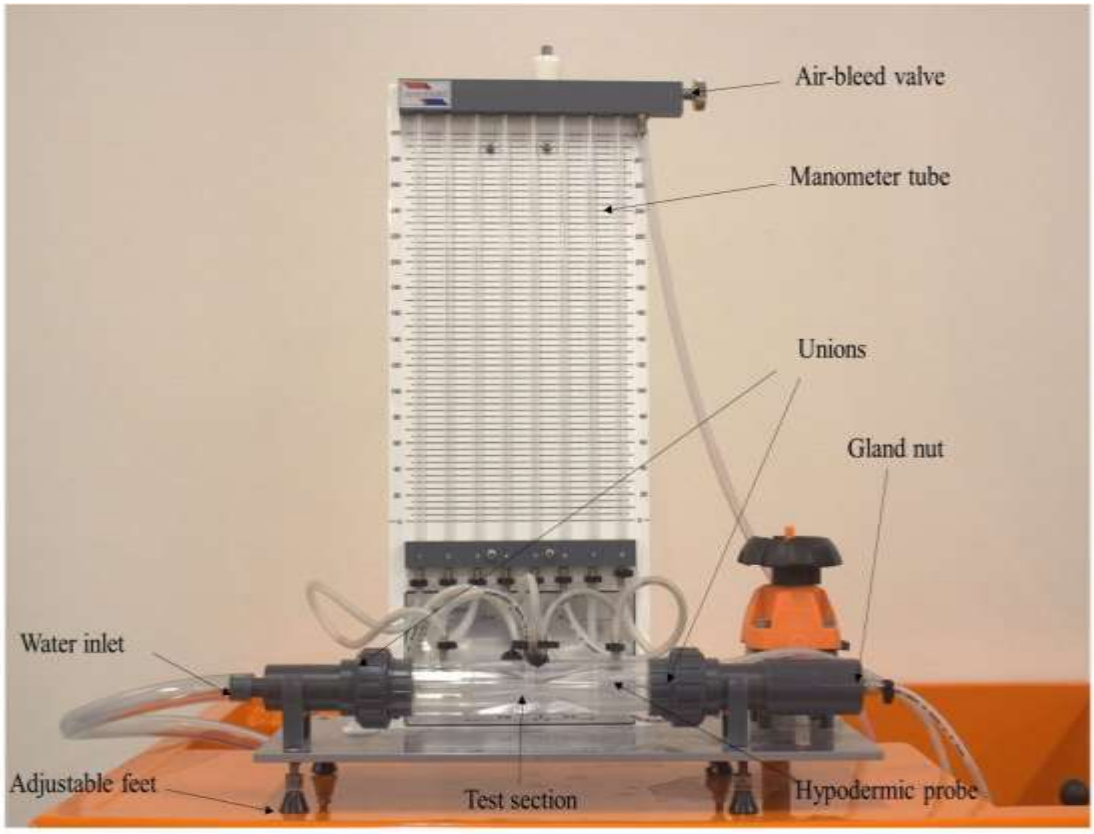

Fig.1 Armfield F1-15 Bernoulli's apparatus test equipment

Manometers make it possible to measure the pressure heads at each of the duct's six sections simultaneously. Fig. 2 displays the test section diameters, tapping locations, and test section dimensions. Two unions—one at each end—are incorporated into the test section to enable reversal for either divergent or convergent testing. A probe is included, which can be positioned at any point along the duct to measure the total pressure head along the test section. After loosening the gland nut, which needs to be manually tightened again, this probe can be moved. The probe was fully inserted during transport and storage to avoid damage. Manometers mounted on a baseboard were connected to the pressure taps. The bench control valve or the apparatus control valve can be used to modify the flow through the test section (Sanghani *et al.,* 2016).

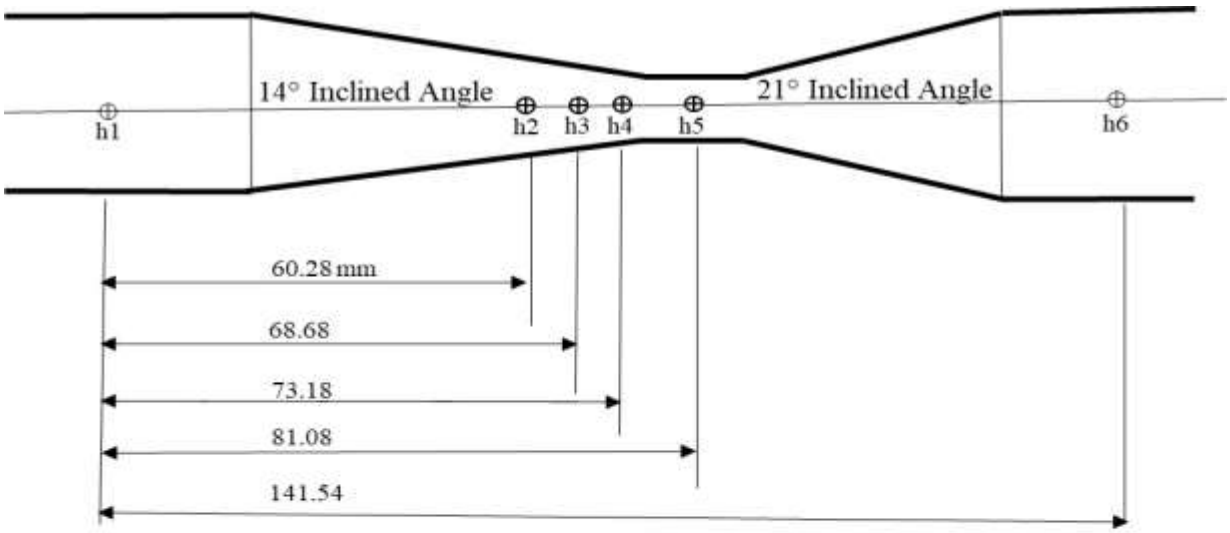

Manometer No.	Test section diameter (mm)
h1	25.0
h2	13.9
h3	11.8
h4	10.7
h5	10.0
h6	25.0

Fig. 2 Test Sections, Manometer Positions, and Diameters of the Duct along the Test Section

C. Venturi Meter

The venturi flow meter is used at the point where there the characteristics change in high velocity and low pressure as depicted in Fig. 3. The pressure dif
ferential, Δh, between the downstream and upstream flows were determined as a function of flow rate. The venturi meter's points and Bernoulli's equation were utilized to connect the flow rate yields to the pressure differential and velocity head of fluid flow.

Assume incompressible flow and no frictional losses, from Bernoulli's Equation;

$$\frac{P_1}{\gamma}+\frac{V_1^2}{2g}+Z_1=\frac{P_2}{\gamma}+\frac{V_2^2}{2g}+Z_2 \quad (1)$$

Use of the continuity Equation $Q = A_1V_1 = A_2V_2$, equation (1) becomes

$$\frac{P_1-P_2}{\gamma}+Z_1-Z_2=\frac{V_2^2}{2g}\left[1-\left\{\frac{A_2^2}{A_1^2}\right\}\right] \quad (2)$$

$$V_2=\frac{1}{\sqrt{\left[1-\left\{\frac{A_2^2}{A_1^2}\right\}\right]}}\sqrt{2g\left[\frac{P_1-P_2}{\gamma}+Z_1-Z_2\right]} \quad (3)$$

Theoretically,

$$Q_{Theoretical} = A_2 V_2 \frac{A_2}{\sqrt{[1-\left\{\frac{A_2^2}{A_1^2}\right\}]}} \sqrt{2g[\frac{P_1-P_2}{\Upsilon} + Z_1 - Z_2]} \quad (4)$$

These two laws and the definition of work and pressure are the basis for Bernoulli's theorem and can be expressed as follows for any two points located on the same streamline in the flow:
where:
P: pressure,
g: acceleration due to gravity,
v: fluid velocity, and
z: vertical elevation of the fluid.
In this experiment, since the duct is horizontal, the difference in height can be disregarded, i.e., $z_1=z_2$

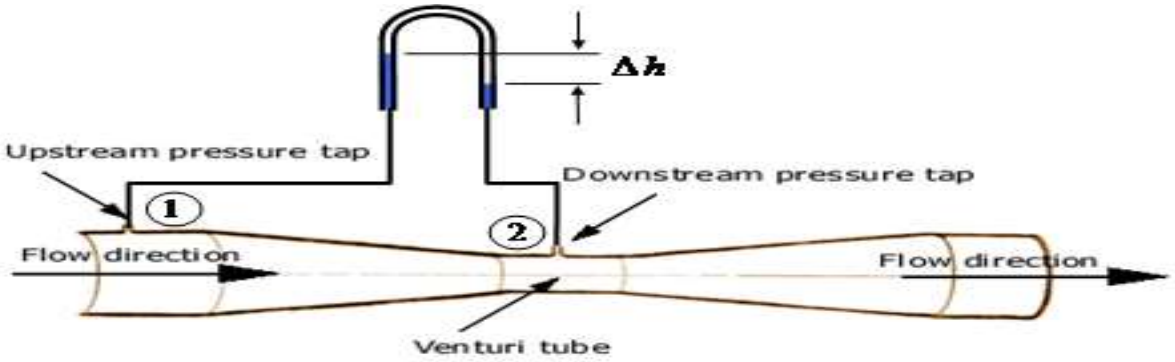

Fig. 3 Venturi meter

D. Venturi and Orifice Flow Meters

These two types of flow meters; venturi and orifice—apply to flow in closed conduits and operate on the principle that if flow velocity increases, pressure must decrease. The flow passes through a pipeline constriction, which causes flow velocity to increase. Figure 4 depicts both types of meters, while Fig. 4 shows the measurement principle.

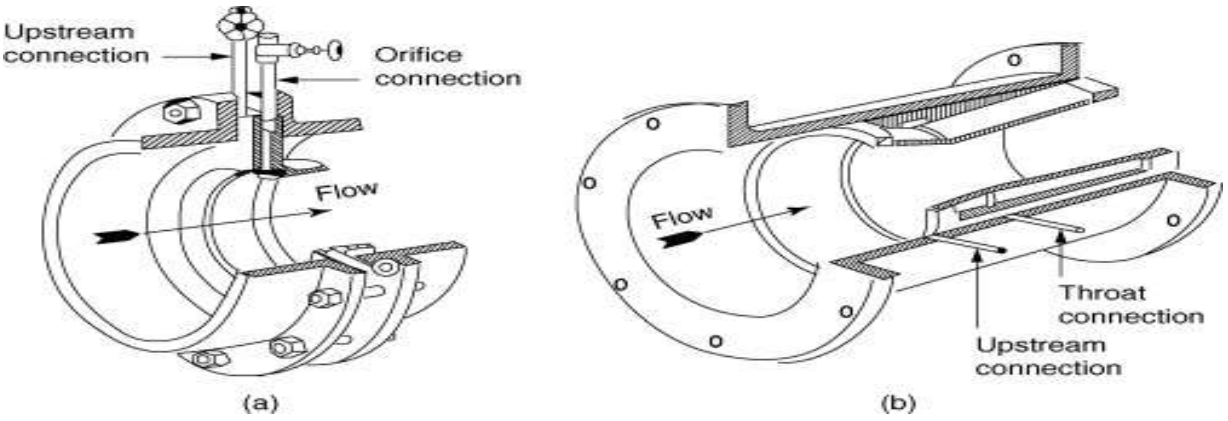

Fig. 4 (a) Orifice metre and (b) Dall type venture metre

E. Dall Tube

Using these flow meter, the pressure drops across the two tapping; one at the throat and the other upstream at the edge of the inlet shoulder was used to evaluate the flowrate in a Dall tube. These meters have permanent pressure losses that are less than those of orifice meters, or even less than those of Venturi tubes, according to some manufacturers. Dall tubes are typically appropriate for measuring the flow rate in medium and large pipe sizes. Depending on the Reynolds number and flowmeter geometry, different flowmeters have different values for Cd. Because of different losses (such as friction losses and area contraction), the discharge coefficient is always lower.

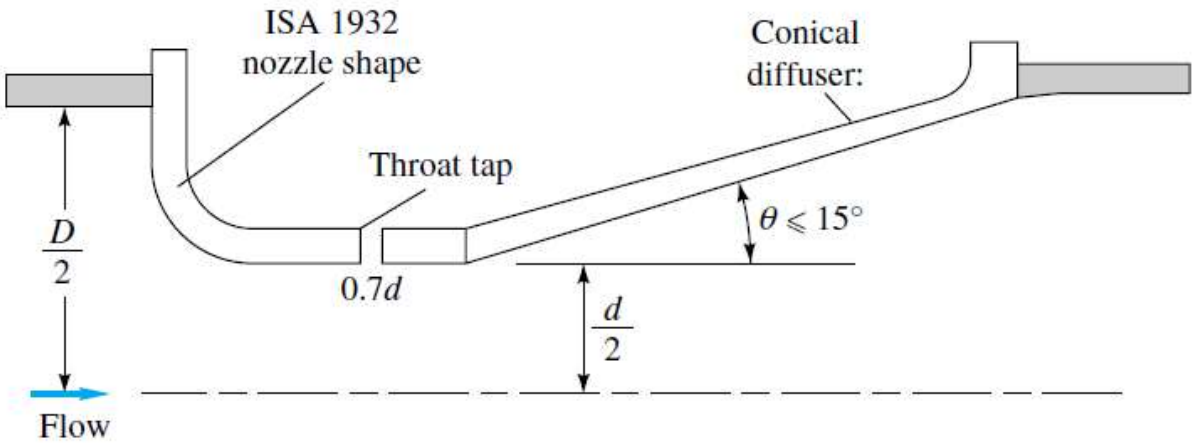

Fig. 5 International standard shapes for venture nozzle

The conical expansion of the modern venturi nozzle, shown in Fig. 5, has a half-angle of no more than 15° and an ISA 1932 nozzle entrance. It is designed to run in the restricted 1.5 x 105 to 2 x 106 Reynolds-number range. The venturi meter's discharge coefficient is between 0.95 and 0.98.

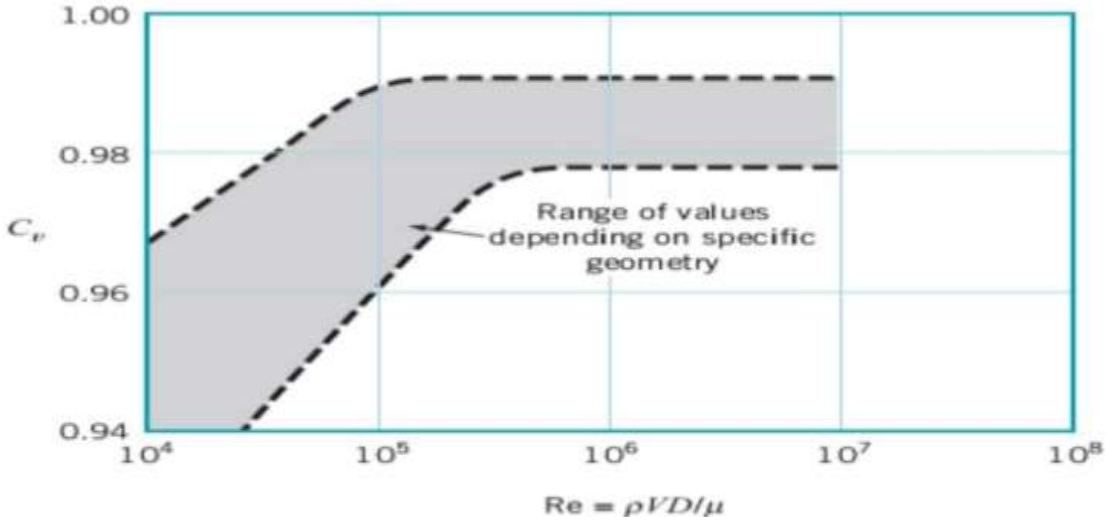

Fig. 6 The co-efficient of discharge of a venturi meter (Archouni *et al.*, 2020)

F. The Orifice Meter

An orifice plate, used as a throttling device, is inserted into the flow to create an orifice meter. There is a discernible pressure differential between the upstream and downstream sides of this orifice plate. The flow rate and this pressure are then connected. The pressure difference changes in direct proportion to the flow rate, just like a Venturi meter does. The construction of the orifice meter is depicted in Fig. 7.

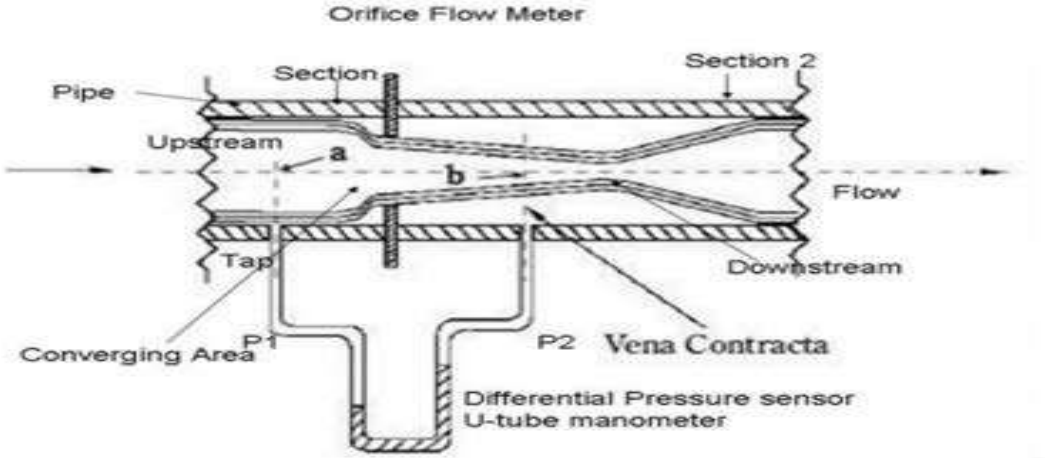

Fig. 7 Cutaway view of the orifice meter

The co-efficient of discharge is 0.62-0.67 for orifice meter.

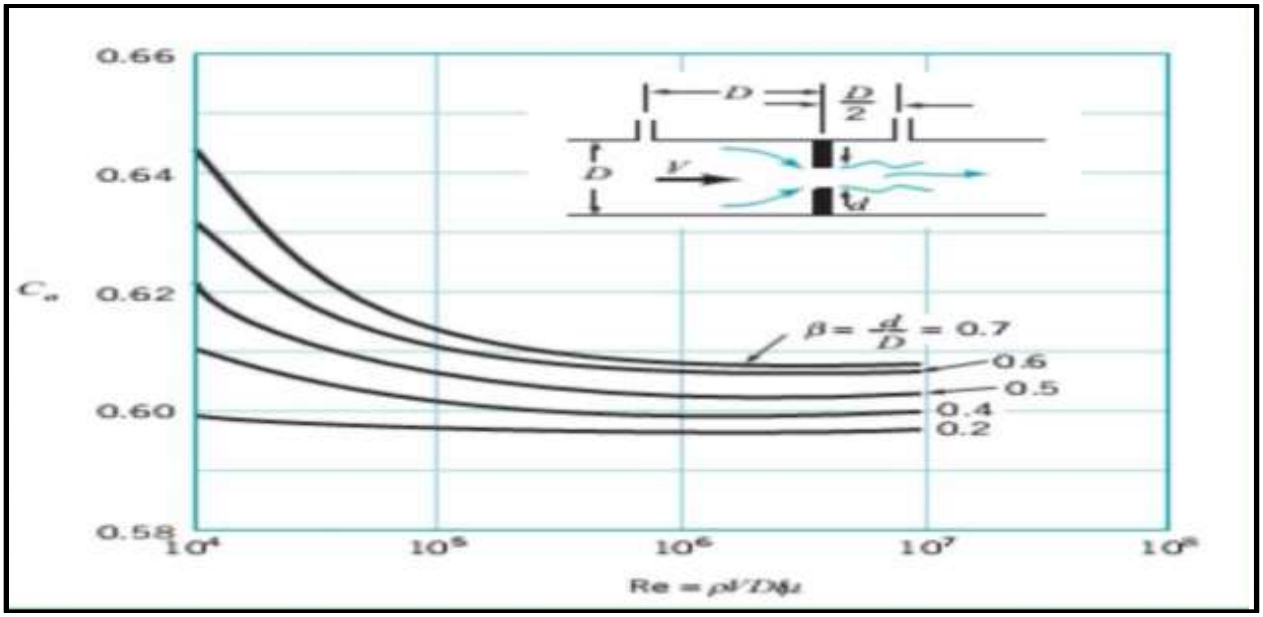

Fig. 8 The co-efficient of discharge of a orifice meter (Padmavathi *et al.,* 2022).

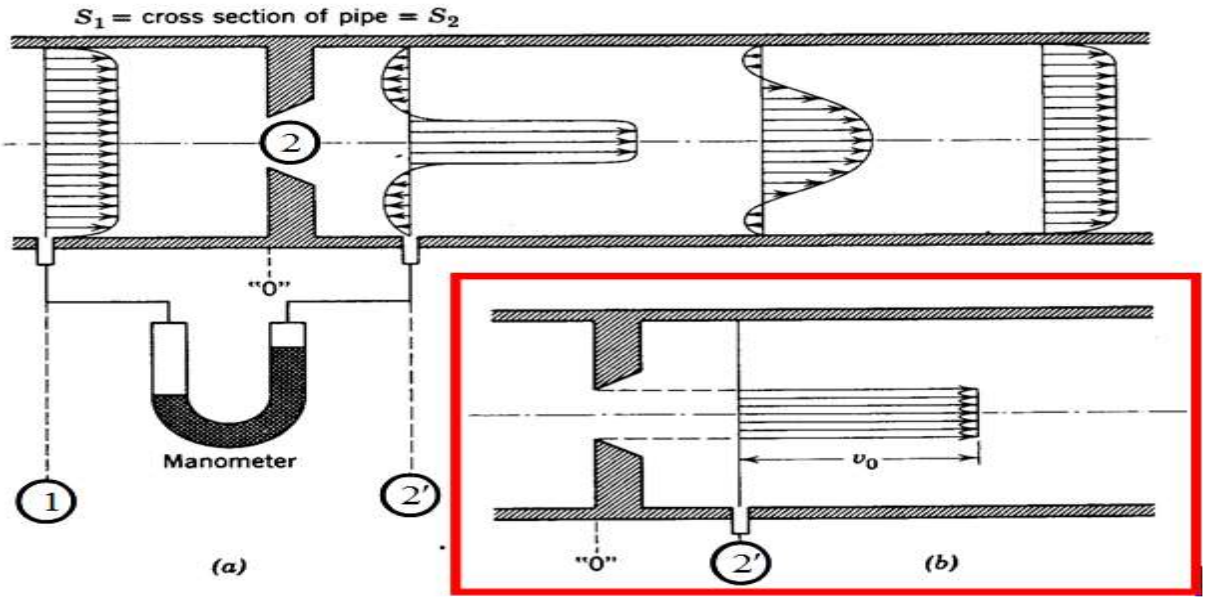

Fig. 9 (a) The approximate velocity profiles at several planes near a sharp-edged orifice plate.

Notably, in extremely turbulent flow, the jet necks down to a minimum cross section at the vena contracta. The jet that emerges from the hole is somewhat smaller than the hole itself. Be aware that some backflow is present close to the wall. (b) The approximate profile displayed is assumed to provide the velocity profile. Furthermore, the uniformity of the velocity profile is assumed. According to boundary layer theory, the pressure of the plug flow is transferred from the plug to the pressure port over the (presumed stagnant) interval.

G. The Variable Area Meter (Rotameter)

A glass tube that gradually tapers is positioned vertically in a frame with its large end facing up to form a rotameter. From below, fluid enters the tube. The float rises to an equilibrium position as it goes in. The equilibrium position is reached when the float's weight is equal to the weight of the fluid it displaces (the buoyant force the fluid applies to the float) and the pressure from velocity (dynamic pressure). The flow rate increases with the float position. When the float is at the tube's top, or at the maximum annular area, maximum flow occurs. Naturally, the minimum area occurs when the float is at the tube's bottom and denotes the minimum flow rate (Jog and Rakesh, 2021).

H. Statistical Analysis

Using SPSS software version 23, a two-way analysis of variance (ANOVA) was performed and compare Means (Paired Samples T-tests) was used to analyze the data. The probability of $P < 0.05$ was used to determine the significance of the differences. To validate the outcomes, the correlation coefficients were calculated using a paired samples correlations techniques in SPSS software version 2023.

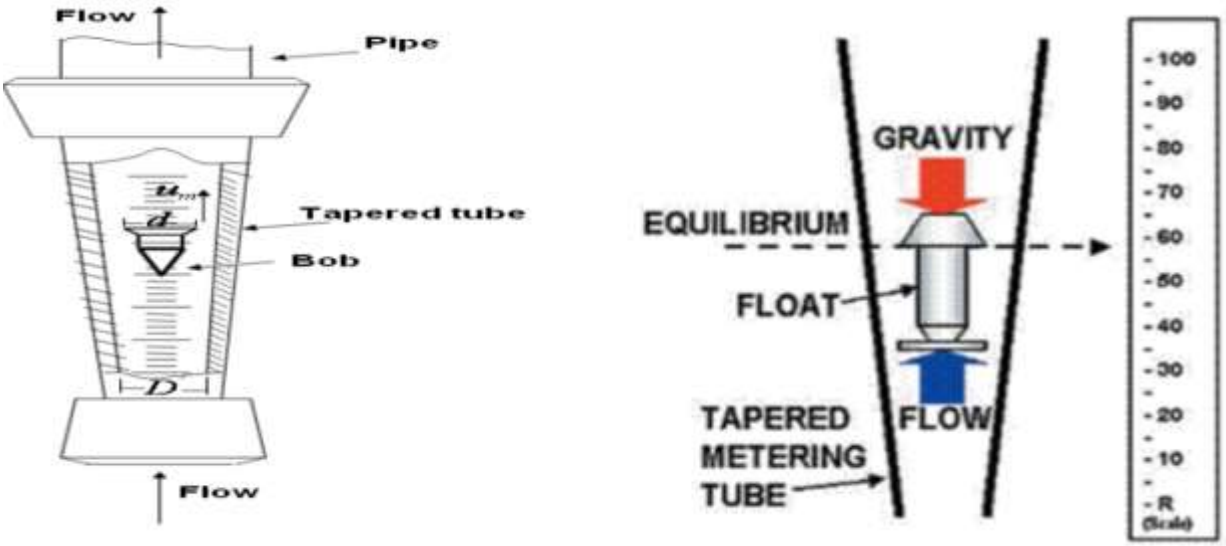

Fig. 8 The Rotameter

RESULTS AND DISCUSSION

In this study, a hydraulic bench, an H5 venturi meter test, and a potential stop watch for time analysis in the flow measurement was utilized at the different pressure variation. Two columns of measurement fluid at various heights are displayed in the venturi meter in the diagram on the left. Each fluid column's height is directly correlated with its pressure. For this reason, in a system where the fluid is moving, static and dynamic pressure are never equal. The source of this pressure differential is a change in fluid velocity, which results in velocity head—a term in the Bernoulli equation that is zero in the absence of fluid bulk motion. Table-1 showed measured flow rate, flow velocity, velocity head, and total head.

Table-1 Measured flow rate, flow velocity, velocity head, and total head, (pressure head+ velocity head)

Position 1: Tapering 14° to 21°

Test Section	Distance into duct (m)	Flow Area (m^2)	Volume (Litre)	Time (sec)	Flow Rate (m^3/s)	Velocity (m/s)	Velocity Head (mm)	Pressure Head (mm)	Total Head (mm)
h_1	0.0000	0.00049	9.5	45.50	0.000209	0.42	9.00	14.70	23.70
h_2	0.06028	0.00015	9.5	37.20	0.000255	1.70	14.70	28.50	43.20
h_3	0.06868	0.00011	9.5	32.40	0.000293	2.66	36.10	32.65	68.75
h_4	0.07318	0.00009	9.5	28.50	0.000333	3.70	69.80	33.60	103.40
h_5	0.08108	0.000079	9.5	24.60	0.000386	4.89	121.80	43.40	165.20
h_6	0.14154	0.00049	9.5	30.30	0.000313	0.64	20.90	15.40	36.30

Fig. 9 shows the graph of fluid parameters (flow rate, velocity, velocity head and pressure head) against time of fluid flow, it was observed that the time of flow varies as the fluid (water) flow from one point to another along the Venturi metre. From the graph, it was also observed that both velocity and pressure head were higher at less flow time.

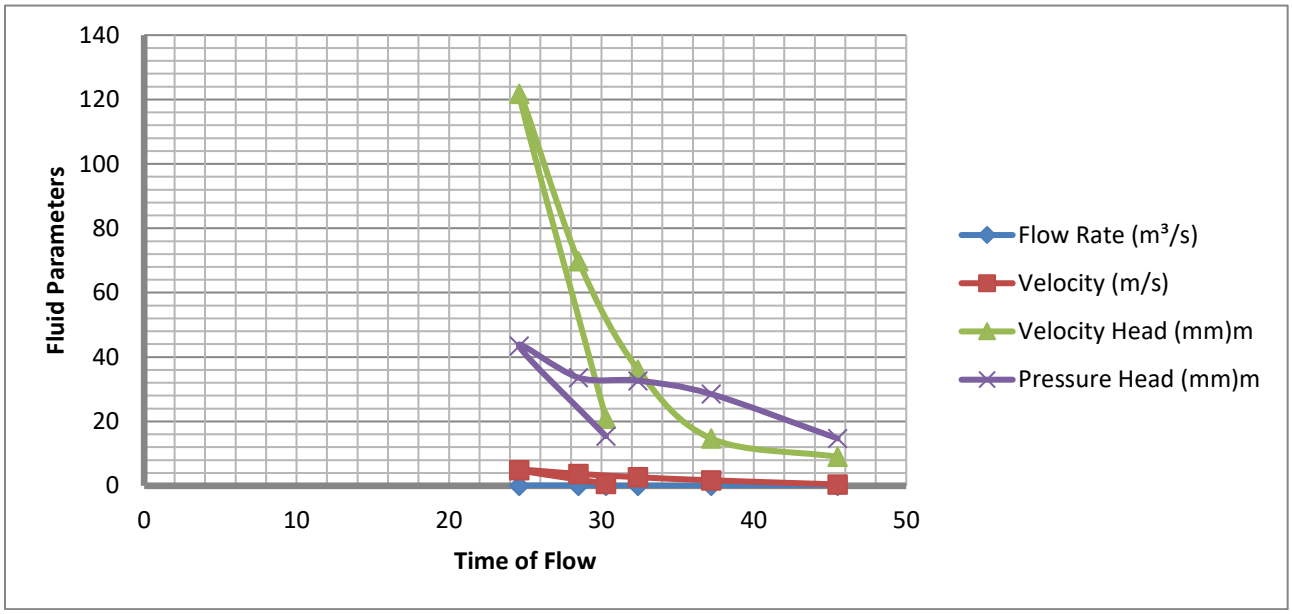

Fig. 9 Graph of fluid parameters (flow rate, velocity, velocity head and pressure head) against time of fluid flow

Compare Means (Paired Samples T-tests)

Table 2 shows that the mean flow rate, velocity, velocity head, pressure head and time of fluid flow were 0.0002982 m³/s, 2.3350m/s, 45.383mm, 28.0417mm and 33.083seconds respectively. Also, Table-2 shows that the fluid parameters such as flow rate, velocity, velocity head and pressure head and time of fluid flow had Standard Error Mean of 0.00002516 m³/s, 0.71741m/s, 17.6885mm, 4.56812mm and, 3.0128seconds respectively. According to Archouni *et al.,* (2020) in their investigation had a Standard Error Mean of 7mm and 6mm for pressure and velocity head respectively. Also, according to Aichouni et al., (2016) obtained mean velocity head and pressure head of 42.25mm, 23.11mm at mean flow rate of 0.0004m³/s. These values obtained by Sanghani *et al.,* (2016) compared favourably to the results obtained in this study.

Table-2 Paired Samples Statistics

	Paired Variables	Mean	N	Standard Deviation	Standard Error Mean
Pair 1	Time (sec.)	33.083	6	7.3798	3.0128
	Pressure Head (mm)	28.0417	6	11.18957	4.56812
Pair 2	Time (sec.)	33.083	6	7.3798	3.0128
	Velocity Head (mm)	45.383	6	43.3278	17.6885

Pair 3	Flow Rate (m^3/s)	0.0002982	6	0.00006163	0.00002516
	Velocity Head (mm)	45.383	6	43.3278	17.6885
Pair 4	Flow Rate (m^3/s)	0.0002982	6	0.00006163	0.00002516
	Pressure Head (mm)	28.0417	6	11.18957	4.56812
Pair 5	Velocity (m/s)	2.3350	6	1.75729	0.71741
	Velocity Head (mm)	45.383	6	43.3278	17.6885
Pair 6	Velocity (m/s)	2.3350	6	1.75729	0.71741
	Pressure Head (mm)	28.0417	6	11.18957	4.56812
Pair 7	Velocity Head (mm)	45.383	6	43.3278	17.6885
	Pressure Head (mm)	28.0417	6	11.18957	4.56812
Pair 8	Time (sec.)	33.083	6	7.3798	3.0128
	Flow Rate (m^3/s)	0.0002982	6	0.00006163	0.00002516
Pair 9	Flow Rate (m^3/s)	0.0002982	6	0.00006163	0.00002516
	Velocity (m/s)	2.3350	6	1.75729	0.71741

Moreover, the significances level in Table-3 ranged from 0.002 to 0.124 which is less than 0.05 at 95% confidence level. The interaction between time & pressure Head, time & velocity head, time & flow rate showed a strong negative correlation of -0.696, -0.790 and -0.980 respectively at significance values of 0.124, 0.061 and 0.001 respectively. While the interaction between flow rate & velocity head, flow rate & pressure head, velocity & velocity head, velocity & pressure head, velocity head & pressure head, time & flow rate, and flow rate & velocity showed a strong positive correlation of 0.885, 0.725, 0.936, 0.966, 0.845 and 0.819 respectively at significance values of 0.019, 0.103, 0.006, 0.002, 0.034 and 0.046 (Table-3). These results show that the flow rate of fluid contributes significantly to both the pressure and velocity head of flow.

Table-3 Paired Samples Correlations

	Paired Variables	N	Correlation	Sig.
Pair 1	Time (sec) & Pressure Head (mm)	6	-0.696	0.124
Pair 2	Time (sec) & Velocity Head (mm)	6	-0.790	0.061
Pair 3	Flow Rate (m^3/s) & Velocity Head (mm)	6	0.885	0.019
Pair 4	Flow Rate (m^3/s) & Pressure Head (mm)	6	0.725	0.103
Pair 5	Velocity (m/s) & Velocity Head (mm)	6	0.936	0.006
Pair 6	Velocity (m/s) & Pressure Head (mm)	6	0.966	0.002
Pair 7	Velocity Head (mm) & Pressure Head (mm)	6	0.845	0.034
Pair 8	Time (sec) & Flow Rate (m^3/s)	6	-0.980	0.001

In addition, Table-4 showed a paired samples test for the interaction of flow rate, velocity, velocity head, pressure head and time of fluid flow which had a significances value which ranged from 0.0001 to 0.568 at 95% confidence level. The value obtained in Table-4 shows that flow rate-velocity head, flow rate-pressure head, velocity-pressure head, time-flow rate, and flow rate –velocity were significant at probability of $P < 0.05$ while other interactions were not significant.

Table-4 Paired Samples Test

	Paired Samples Test								
	Paired Variables	Paired Differences					t	df	Sig. (2-tailed)
		Mean	Std. Deviation	Std. Error Mean	95% Confidence Interval of the Difference				
					Lower	Upper			
Pair 1	Time (sec) - Pressure Head (mm)	5.04167	17.16591	7.00795	-12.97285	23.05618	0.719	5	0.504
Pair 2	Time (sec) - Velocity Head (mm)	-12.3000	49.3687	20.1547	-64.1093	39.5093	-0.610	5	0.568
Pair 3	Flow Rate (m^3/s) - Velocity Head (mm)	-45.38303517	43.32778485	17.68849410	-90.85275679	0.0866864 6	-2.566	5	0.050
Pair 4	Flow Rate (m^3/s) - Pressure Head (mm)	-28.04136850	11.18952261	4.56810348	-39.78405232	-16.29868468	-6.139	5	0.002
Pair 5	Velocity (m/s) - Velocity Head (mm)	-43.04833	41.68818	17.01913	-86.79739	0.70073	-2.529	5	0.053
Pair 6	Velocity (m/s) - Pressure Head (mm)m	-25.70667	9.50210	3.87922	-35.67851	-15.73482	-6.627	5	0.001
Pair 7	Velocity Head (mm) - Pressure Head (mm)	17.34167	34.40256	14.04479	-18.76161	53.44494	1.235	5	0.272
Pair 8	Time (sec) - Flow Rate (m^3/s)	33.08303517	7.37987518	3.01282142	25.33833114	40.82773920	10.981	5	0.000
Pair 9	Flow Rate (m^3/s) - Velocity (m/s)	-2.33470183	1.75724008	.71739026	-4.17881220	-0.49059147	-3.254	5	0.023

Also, Fig. 10 shows an error bar plot for rate of flow, velocity head, and pressure head. It was observed that an error bar was present in six plots out of thirty-six plots, covering 16.7% of the total plot. This indicates that 83.3% of the experimental values are error free. The results of this study demonstrate a strong correlation between flow rate, pressure variation, and velocity at various cross-sectional areas of the fluid transportation piping system, particularly in the oil and gas sector. This is consistent with research by Archouni *et al.* (2020) on the experimental investigation of the effects of installations on the performance of venturi flow meters, which also demonstrates that a venturi flow meter's total head is significantly influenced by the flow rate.

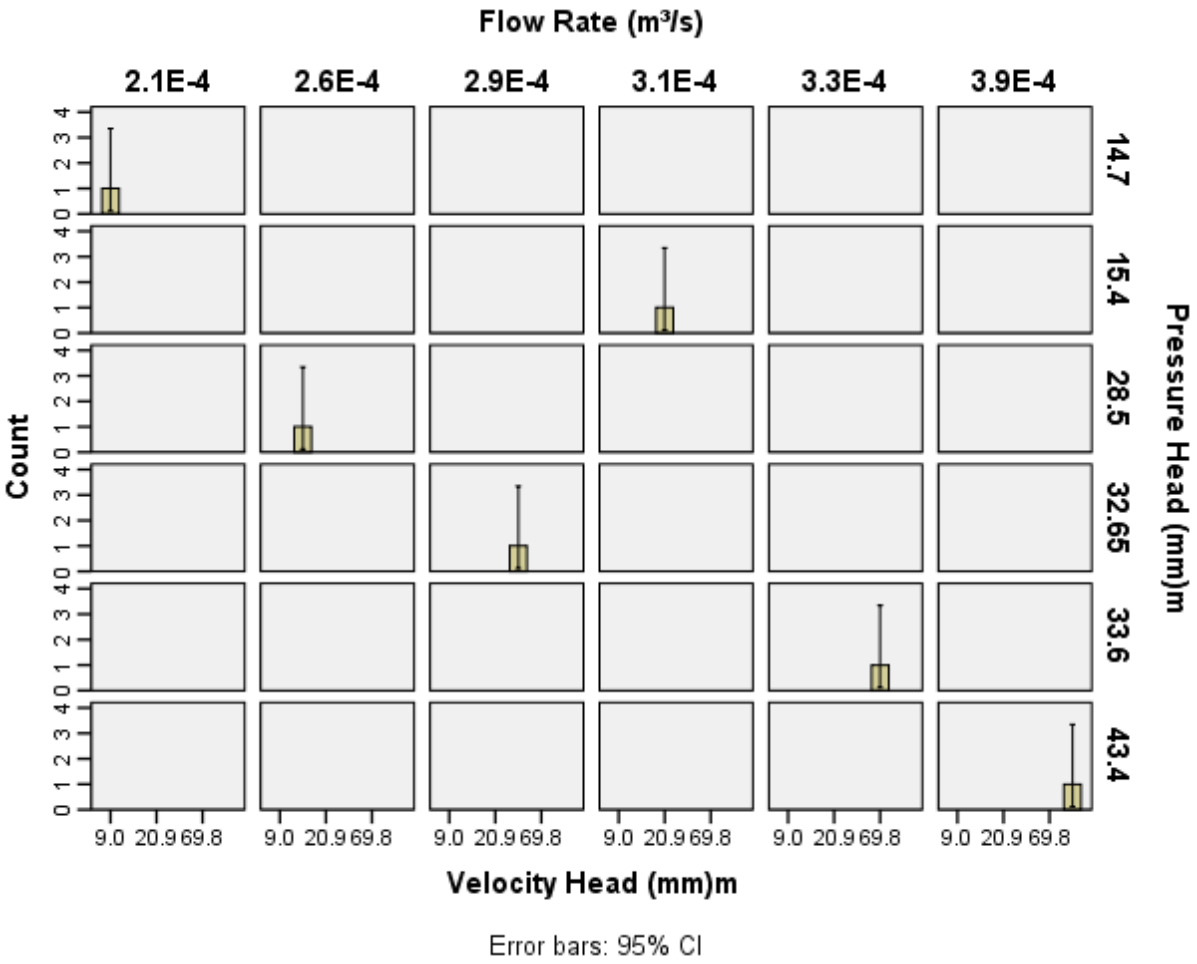

Fig. 10 Error Bar Plot for Rate of Flow, Velocity Head, and Pressure Head

CONCLUSION

The investigation of the effects of flow rate on velocity and pressure head using venturi flow meter has been achieved. Paired Samples Test for the interaction of flow rate, velocity, velocity head, pressure head and time of fluid flow had a significances value which ranged from 0.0001 to 0.568 at 95% confidence level. The value obtained shows that Flow Rate-velocity head, flow rate-pressure head, velocity-pressure head, time-flow rate, and flow rate–velocity were significant at probability of $P < 0.05$ while other interaction were not significant. The venturi meter analyses show the relationship between pressure

losses, variation of pressure and velocity at different cross-sectional area of the piping system used in transportation of fluid especially in the oil and gas industry.

ACKNOWLEDGMENTS

The authors acknowledged the Department of Mechanical Engineering, Faculty of Engineering, Benson Idahosa University for the using some of their facilities during the fabrication process.

CONFLICT OF INTEREST

There is no conflict of interest among the authors.

REFERENCE

Archouni M., Retiel N., Nehari D., Laribi B., Houat, S. and Benchicou S. (2020). Experimental Investigation of the Installations Effects on the Venturi Flow Meter Performance, Proceedings of the FEDSM2000 ASME Fluid Engineering Conference, June 11-15, Boston, USA.

Aichouni M., Laws E.M., and Ouazzane A.K. (2016). Experimental Study of the Effects of Upstream Flow Condition upon Venturi Flow Meter Performance, Journal of Fluid Mechanics, 13(2); 10-17.

Demirkesen C., Colak U., Savci I. H., and Zeren, H.B. (2020). Experimental and Numerical Investigation of Air Flow Motion in Cylinder of Heavy-Duty Diesel Engines, *Journal of Applied Fluid Mechanics,* 13(2); 537-547.

Deo S., and Tiwari A., (2008). On The Solution of a Partial Differential Equation Representing Rotational Flow in Bispherical Polar Coordinates, *Applied Mathematical Computation,* 205(1): 475–477.

Elperin T., Fominykh A., Klochko M. (2012). Performance of a Venturi Meter in Gas–Liquid Flow in the Presence of Dissolved Gases, Flow Measurement and Instrumentation, 13(1): 13-16.

Gupta S., Poulikakos D., and Kurtcuoglu V. (2018). Analytical Solution for Pulsatile Viscous Flow in a Straight Elliptic Annulus and Application to the Motion of the Cerebrospinal Fluid, *Phys. Fluids,* 31(9): 1-12.

Guria M., Jana R.N., and Ghosh S.K. (2016). Unsteady Flow in a Rotating System. *International Journal Non-linear Mechanics*, 41(6): 838–843.

Hall O., Gilbert A.D., and Hills C.P., (2017). Converging Flow between Coaxial Cones. *Fluid Dynamic Research*, 62(1): 1-25.

Jog C.S., and Rakesh K. (2021). Shortcomings of Discontinuous-Pressure Finite Element Methods on a Class of Transient Problems, *International Journal of Numerical Mathematics of Fluids*, 82(3): 313–326.

Joseph D.D. (2018). Potential Flow of Viscous Fluids: Historical Notes. *International Journal of Multiphase Flow*, 32(3): 285–310.

Muhammad G.N. Shah A., and Mushtaq M. (2021). Indirect Boundary Element Method for Calculation of Potential Flow Around a Prolate Spheroid, *Journal of American Science*, 23(3): 148–156.

Padmavathi B.S., Rajashekhar G.P. and Amarnath T. (2022). A Note on Complete General Solutions of Stokes Equations, Quart. *Journal Mechanical Applied Mathematics,* 74(3): 383–388.

Sanghani C.R. Jayani D.C., Jadvani N.R. Dobariya H.N., Jasoliya K.R. (2016). Effect of Geometrical Parameters of Venturi Meter on Pressure Drop. *Themed Section: Engineering and Technology*, 2(2): 865-868.

Shinde P.R., Chaudhari R.H., Patil P.S., Marathe S.S. (2020). Modeling and Simulation of Venturi Parameters in Relation to Geometries and Discharge Coefficient with Computational Fluid Dynamics Technique, *International Journal of Engineering Research & Technology,* 9(5): 681-687.